

RESEARCH ARTICLE

Open Access



# The size of via holes influence the amplitude and selectivity of neural signals in Micro-ECoG arrays

Manan Sethia and Mesut Sahin\*

## Abstract

**Background:** Electrocorticography (ECoG) arrays are commonly used to record the brain activity both in animal and human subjects. There is a lack of guidelines in the literature as to how the array geometry, particularly the via holes in the substrate, affects the recorded signals. A finite element (FE) model was developed to simulate the electric field generated by neurons located at different depths in the rat brain cortex and a micro ECoG array ( $\mu$ ECoG) was placed on the pia surface for recording the neural signal. The array design chosen was a typical array of  $8 \times 8$  circular ( $100 \mu\text{m}$  in diam.) contacts with  $500 \mu\text{m}$  pitch. The size of the via holes between the recording contacts was varied to see the effect.

**Results:** The results showed that recorded signal amplitudes were reduced if the substrate was smaller than about four times the depth of the neuron in the gray matter. The signal amplitude profiles had dips around the via holes and the amplitudes were also lower at the contact sites as compared to the design without the holes; an effect that increased with the hole size. Another noteworthy result is that the spatial selectivity of the multi-contact recordings could be improved or reduced by the selection of the via hole sizes, and the effect depended on the distance between the neuron pair targeted for selective recording and its depth.

**Conclusions:** The results suggest that the via-hole size clearly affects the recorded neural signal amplitudes and it can be leveraged as a parameter to reduce the inter-channel correlation and thus maximize the information content of neural signals with  $\mu$ ECoG arrays.

**Keywords:** Multi-electrode arrays, Perforation holes, Channel crosstalk

## Background

$\mu$ ECoG arrays can, for instance, monitor brain cortical activity in experimental animals, and localize the seizures in epilepsy patients, without penetrating the brain parenchyma. They are commercially available with metal contacts with varying sizes, inter-contact distances (pitch), and number of contacts on non-conductive substrate materials such as silicone, parylene-C, or polyimide [1]. Perforating via holes through the substrate are

usually incorporated into the design to allow simultaneous recordings with penetrating microelectrodes [2] or injection of drugs [3]. However, the electrode array design is mostly based on personal experience of the investigator and putative design criteria that are believed to be the best match to the application in consideration. There is clearly a need for better guidelines as to how the array geometry affects the recorded signals. We hypothesized that the size of the via holes in particular must make a significant effect on the recorded signal amplitudes and perhaps on spatial selectivity since they provide passages of high electrical conductivity through

\* Correspondence: [sahin@njit.edu](mailto:sahin@njit.edu)

Biomedical Engineering Department, New Jersey Institute of Technology, Newark, NJ 07102, USA



© The Author(s). 2022 **Open Access** This article is licensed under a Creative Commons Attribution 4.0 International License, which permits use, sharing, adaptation, distribution and reproduction in any medium or format, as long as you give appropriate credit to the original author(s) and the source, provide a link to the Creative Commons licence, and indicate if changes were made. The images or other third party material in this article are included in the article's Creative Commons licence, unless indicated otherwise in a credit line to the material. If material is not included in the article's Creative Commons licence and your intended use is not permitted by statutory regulation or exceeds the permitted use, you will need to obtain permission directly from the copyright holder. To view a copy of this licence, visit <http://creativecommons.org/licenses/by/4.0/>. The Creative Commons Public Domain Dedication waiver (<http://creativecommons.org/publicdomain/zero/1.0/>) applies to the data made available in this article, unless otherwise stated in a credit line to the data.

a non-conductive substrate that forms an electrical barrier between the two sides of the array.

### Inter-Channel correlation

Several reports investigated the effects of contact spacing and size on the spatial selectivity of neural recordings. In a comparative study with  $\mu$ ECoG recordings, the inter-channel correlation was found to be highly dependent on inter-contact distance and frequency of interest both in anesthetized human subjects and mice [4]. The smaller contact pitch with  $\mu$ ECoG arrays (1.68 mm and 3 mm, in minipigs) was found to be instrumental for localization of the regions of evoked activity that were less than 1 cm apart, which would have not been possible with conventional ECoG electrodes [5]. On the other hand, a brain-computer interface (BCI) study in macaques concluded that the decoding performance decreased and inter-channel cross correlations increased when contact pitch was reduced from 9 mm to 3 mm [6]. Using FE models, the minimum contact pitch for high spatial selectivity was estimated to be 0.6 mm and 1.7 mm for the rat and human brains respectively for subdural placements of the arrays and using 10% of the max as a threshold to determine the spatial spread of the voltage [7].

### Signal amplitude and frequency content

Rigorous metrics were developed for comparing the quality of neural signals recorded with  $\mu$ ECoG arrays in terms of their signal-to-noise ratio and frequency content [8]. A study conducted in resting human subjects showed that the  $\mu$ ECoG arrays (75  $\mu$ m contact diameter with 1 mm pitch) had significantly higher amplitudes and higher frequency components when the arrays were placed subdurally, compared to epidural placements, although the difference was negligible with macro ECoG arrays (2 mm contact diameter with 1 cm pitch) [9]. Subdural placement of  $\mu$ ECoG arrays recorded frequency components up to 800 Hz on the rat cerebellar cortex where the inter-contact coherence increased substantially in transitioning from anesthesia to the awake state, whereas the frequency band from the motor cortex was limited to 200 Hz [10, 11], suggesting that the frequency content of the  $\mu$ ECoG signals can vary substantially depend on the brain site and state.  $\mu$ ECoG arrays with 100  $\mu$ m contacts could detect multi-unit activity on the auditory cortex of guinea pigs [12]. It was also suggested that  $\mu$ ECoG arrays cause less surgical complications during implantation than macro-ECoG due to their smaller size [13].

Although numerous reports looked at the effects of contact spacing and size on the recorded neural signal amplitudes, and spatial selectivity using both experimental data and FE analysis, as reviewed above, there is no

significant study that systematically investigated the effects of perforating holes in the substrate that are commonly included in the  $\mu$ ECoG designs, and the size of the substrate itself on the recorded signals. Computer simulations allow investigation of a large number of design variations in a reproducible manner free from uncontrollable perturbations and noise commonly seen in experimental setups, such as anatomical variations and differences in the implant quality between subjects. On the other hand, computer simulations may fall short of mimicking actual scenarios due to a lack of realistic values for specific conductivities of different tissue compartments, and due to local inhomogeneities that the computer models usually have to ignore to keep the computation time manageable. Nonetheless, the principles learned here and the underlying mechanisms should prevail across different  $\mu$ ECoG designs although quantitative results may vary. In this paper, we used an FE model to gain some basic understanding of how the substrate size and the size of the via holes affect the amplitudes and spatial selectivity of the signals recorded from neurons located in the gray matter of a rat brain.

### Methods

A FE model was developed on COMSOL Multiphysics v5.4 platform. The model was designed to mimic a rat brain in terms of layer thicknesses and their electrical conductivities taken from the literature (1). The model was divided into ten isotropic layers representing air, scalp, skin, skull, dura mater, arachnoid, sub-arachnoid or cerebrospinal fluid (CSF), pia mater, gray matter and the white matter (Table 1). The  $\mu$ ECoG electrode design was constructed with typical parameters (Table 2) commonly used in commercially available  $8 \times 8$  arrays for animal experiments [14, 15]. The contacts were 100  $\mu$ m in diameter with a pitch of 500  $\mu$ m (Figs. 1 & 2) placed on a polyimide substrate with a thickness of 20  $\mu$ m. As it is commonly included in the  $\mu$ ECoG array designs, via holes with varying sizes (20  $\mu$ m, 50  $\mu$ m, and 200  $\mu$ m) were introduced into the substrate at the geometric center of each set of four neighboring contacts (Fig. 2). A neuron was modelled using a dipole current source with a magnitude of 1  $\mu$ A and a separation of 50  $\mu$ m, and vertically positioned at one of the three different depths; 500  $\mu$ m, 1000  $\mu$ m, and 1500  $\mu$ m, from the pia surface. Note that 1  $\mu$ A was adopted here as a generic value, and not intended to mimic the membrane current of a specific type of a neuron. Thus, the voltages reported here should be considered as relative numbers with respect to 1  $\mu$ A source current. Voltage profiles were simulated also for the cases of no via holes and in the absence of an electrode substrate for comparison.

Boundary conditions were applied to the model by assigning ground terminal to all the outer boundaries

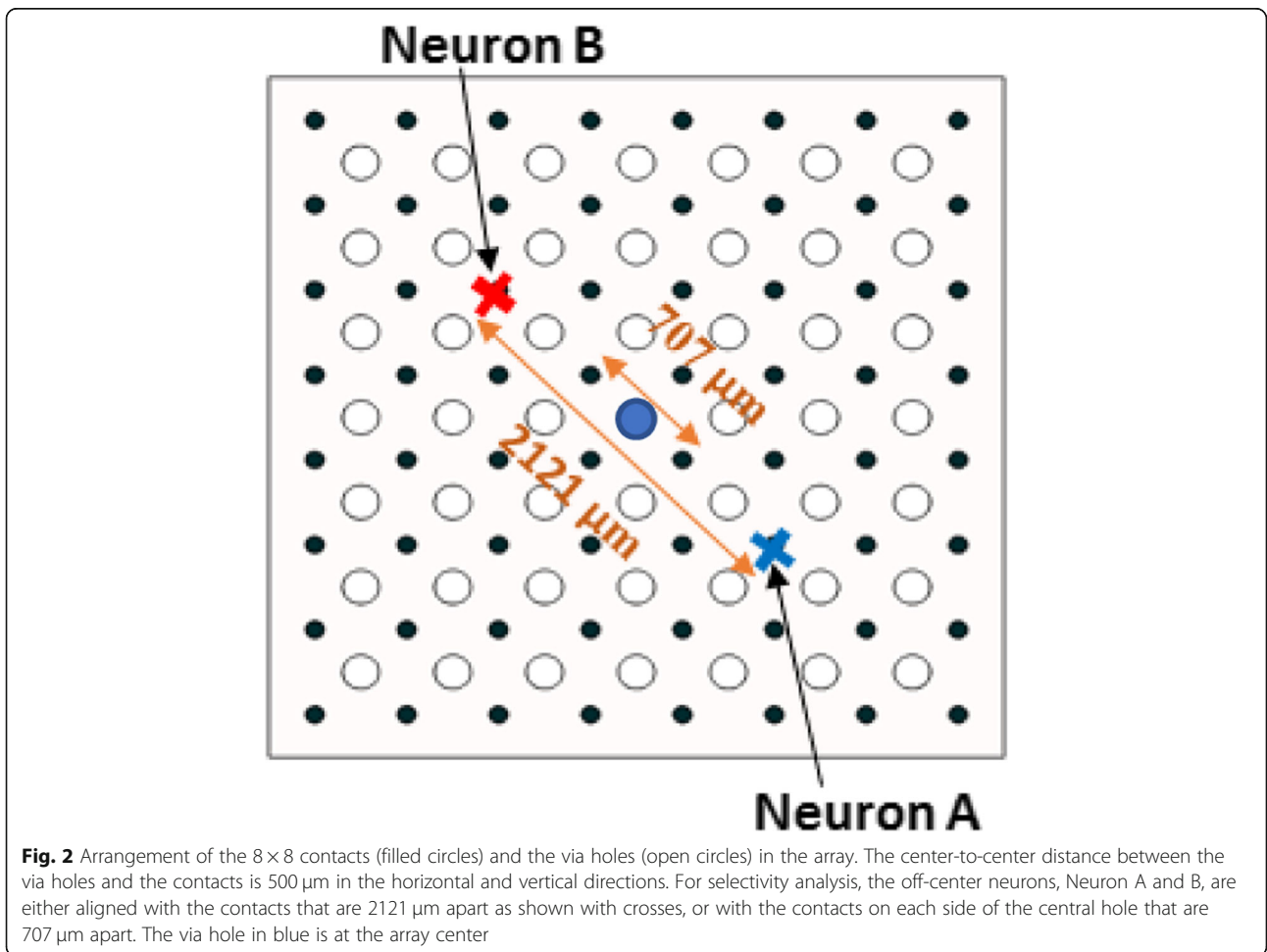
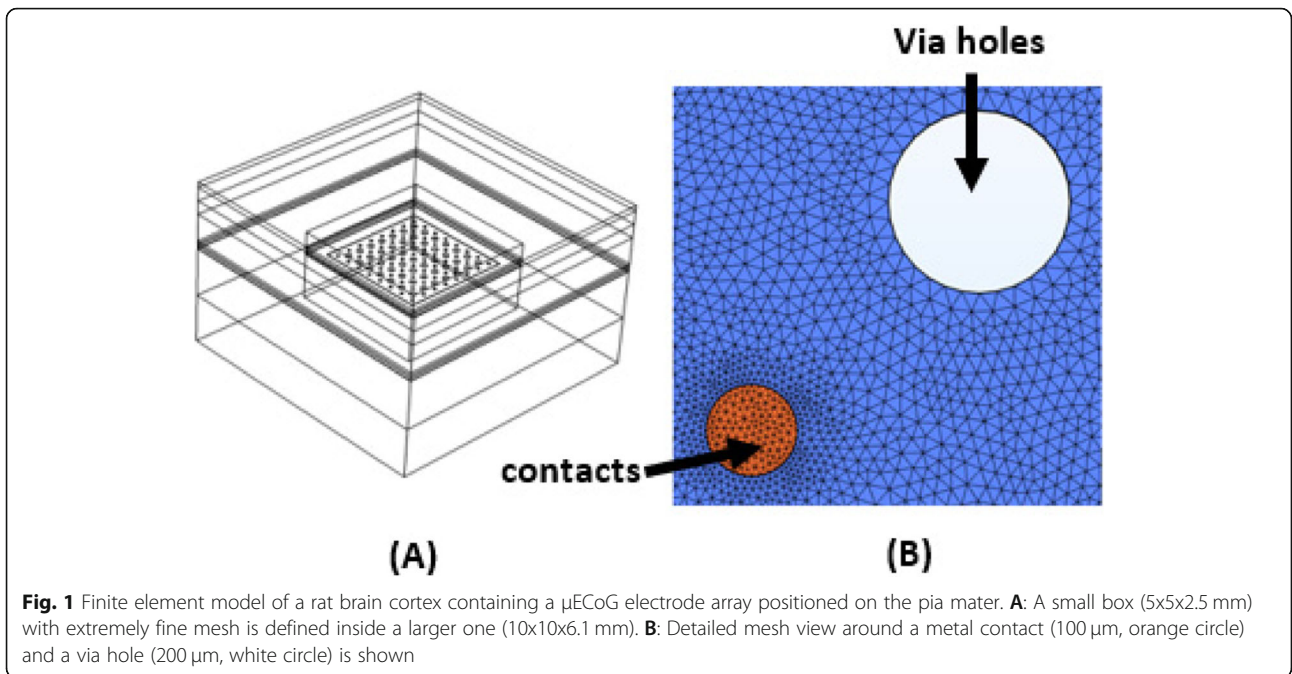


**Table 1** Thicknesses and electrical conductivities for the cortical layers included in the rat brain model

Rat Brain Model			
Layer	Thickness ( $\mu\text{m}$ )	Specific conductivity (S/m)	References
Air	100	$1 \times 10^{-15}$	
Scalp	500	0.2	Geddes and Baker 1967
Skin	500	0.05	
Skull	1000	0.02	Kosterich et al.
Dura	100	0.03	Struijk et al., 1997
Arachnoid	75	0.03	
CSF	100	1.8	Baumann et al., 1997
Pia	25	0.23	
Gray	1800	0.23	Latikka et al., 2001
White	1800	0.6	Ranck and Bement, 1965

except the top surface, which was by default assigned as an insulator (air). A smaller cubical box (5x5x2.5 mm) was constructed containing the  $\mu\text{ECoG}$  array and the neuron, and was set to “extremely fine” level of mesh (element size 2  $\mu\text{m}$ ). The middle four layers from the pia to dura were set to “extra fine” mesh (element size 15  $\mu\text{m}$ ) and the gray matter outside the small box, the white matter, and the top four layers were set to “finer” mesh (element size 40  $\mu\text{m}$ ). The model consisted of  $\sim$  11.6 million domain and boundary elements, and the simulation time was  $\sim$  1 h 20 min on a i5-8265U dual-core CPU running at 1.60GHz and 1.80 GHz with 8 GB RAM. Voltages computed at all the elements of the 3D COMSOL model were exported to Matlab (Mathworks Inc.) and voltage profiles next to the bottom surface of the substrate were plotted. The presence of the metal contacts made small differences in the voltage profiles. The voltage at any point underneath the array could also be thought of as a voltage measurement point from an infinitely small contact hypothetically located at that point. We noticed that electric fields at the vicinity of

**Table 2** Material properties and geometric parameters of the  $\mu\text{ECoG}$  array

$\mu\text{ECoG}$ array design		
Contacts platinum/ iridium ( $4 \times 10^6 \text{S/m}$ )	contact diam.	100 $\mu\text{m}$
	contact pitch	500 $\mu\text{m}$
	No. of contacts	$8 \times 8$ contacts
Substrate polyimide ( $6.67 \times 10^{-16} \text{S/m}$ )	substrate dimensions	$0.5 \times 0.5 \text{ mm}$ 1 $\times$ 1 mm 2 $\times$ 2 mm 4 $\times$ 4 mm
	thickness	20 $\mu\text{m}$

the contacts had significant computational errors due to sharp transitions in conductivity in a span of a few microns. Thus, for accurate calculations of spatial selectivity, the contacts were removed from the model and the voltages were taken where the contacts were located in the original model. In real electrodes, the presence of the contacts will not affect the voltage field to the degree predicted by the FE model because of the electrode-electrode interface impedance distributed across the contact surface.

When contacts were present, the voltage profiles made across the array were sampled at 10  $\mu\text{m}$  below the array surface to avoid these transitional effects.

A neuron was placed beneath the central via hole at varying depths for initial amplitude analysis (Fig. 2). For selectivity analysis, two neurons symmetrically positioned along the array’s diagonal axis and with varying depths were introduced to the model. Spatial selectivity is the ability of an electrode to record preferentially higher signals from one neuron vs. another at a different location. For example, Neuron A positioned precisely below the recording contact will induce a higher amplitude signal on this contact compared to another neuron (Neuron B) placed farther away (Fig. 2). Thus, spatial selectivity (SS) is defined as the ratio of the potential difference between the voltages induced by those two neurons to the voltage of the neuron that is located closer to the recording site. A SS value of 1 represent perfect selectivity where  $V_B$ , signal from Neuron B, is zero.

$$SS = \frac{V_A - V_B}{V_A} \quad (1)$$

## Results

As expected, the voltage field of the neuron, simulated as a dipole current source, drops exponentially by distance (Fig. 3). Near zero potentials are measured (dark blue areas) in regions where the anodic and cathodic fields from the dipole cancel each other.

The voltage field spreads further above the neuron than it does below it due to the presence of a low-conductivity skull and the non-conductive air above the scalp. The electrode array also blocks the vertical flow of the current, which further reduces the voltage gradient (rate of decrease) in the vertical direction.

In order to demonstrate the effect that the presence of a non-conductive substrate makes on the recorded voltages, the voltage profiles at the substrate bottom surface were plotted for different substrate sizes (Fig. 4). The voltage amplitudes increased under the array and decreased outside the substrate compared to the no-substrate case (blue trace). Consequently, the voltage

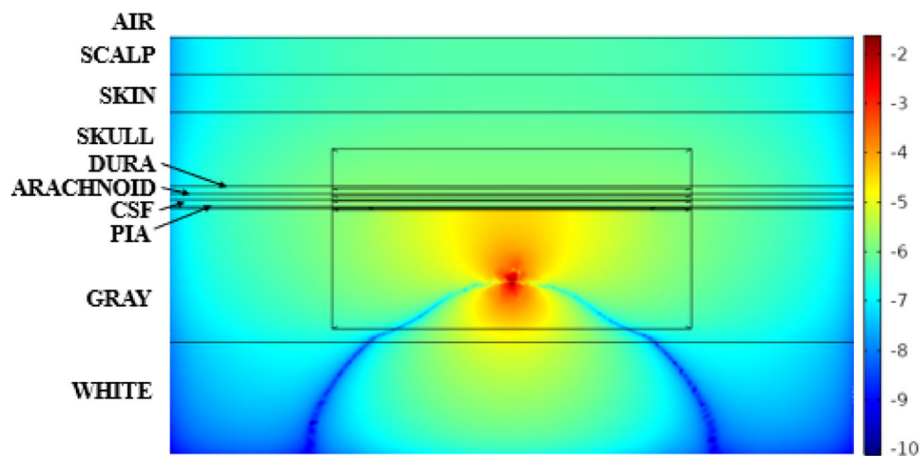


**Fig. 3** Voltage field in a vertical plane that cuts through the center of the model. Absolute values of the voltages are plotted on a logarithmic scale shown on the right. The neuron is located where the maximum voltages are observed. The small box delineates the region with extremely fine mesh containing the array and the neuron. Both positive (above the neuron) and negative (below the neuron) voltages are shown on the same color scale using the absolute values

profiles had sharp slope changes at the edges of the substrate. The peak voltage increased significantly with the substrate size and reached to  $\sim 34 \mu\text{V}$  for the  $4 \times 4 \text{ mm}$  array (green trace), which was larger than twice the voltage recorded in the absence of the array ( $16 \mu\text{V}$ , blue trace). The peak voltage for a  $10 \times 10 \text{ mm}$  substrate (not shown) was close to that of  $4 \times 4 \text{ mm}$ , indicating a plateau effect. For the substrate size of  $1 \times 1 \text{ mm}$ , which is in the same order as the

neuron depth in this case ( $1000 \mu\text{m}$ ), the voltage ( $26.8 \mu\text{V}$ ) increase was about 68% compared to the no-substrate case, and 21% less than the voltage measured with the largest substrate ( $34 \mu\text{V}$ ). These simulations suggest that the presence of a non-conductive array substantially impacts the voltages recorded at the array, especially when the substrate size is a few times larger than the depth of the neuron that is acting as the source.

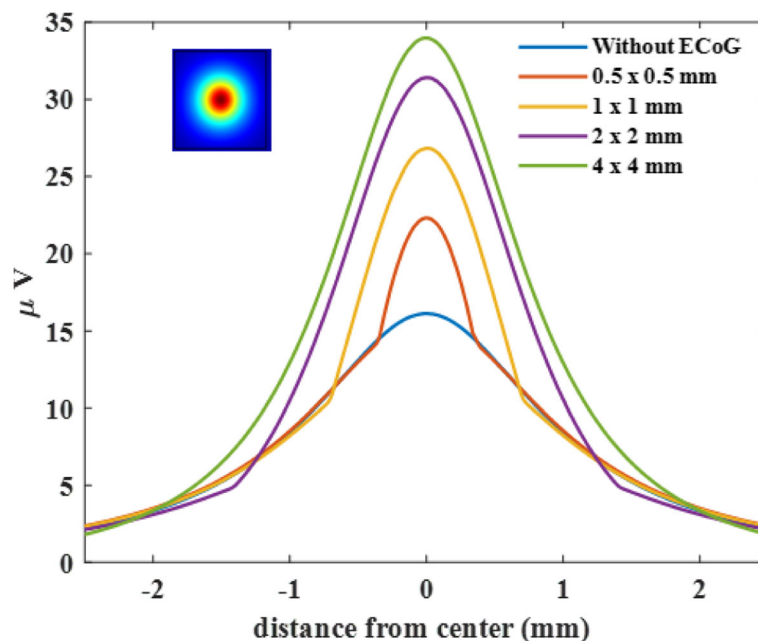


**Fig. 4** Voltage profile along the diagonal axis beneath the electrode array for varying substrate sizes as well as in the absence of a substrate. The recorded voltage increases with array size. The neuron is at a depth of  $1000 \mu\text{m}$  from the pia surface and aligned with the center of the array. No via holes

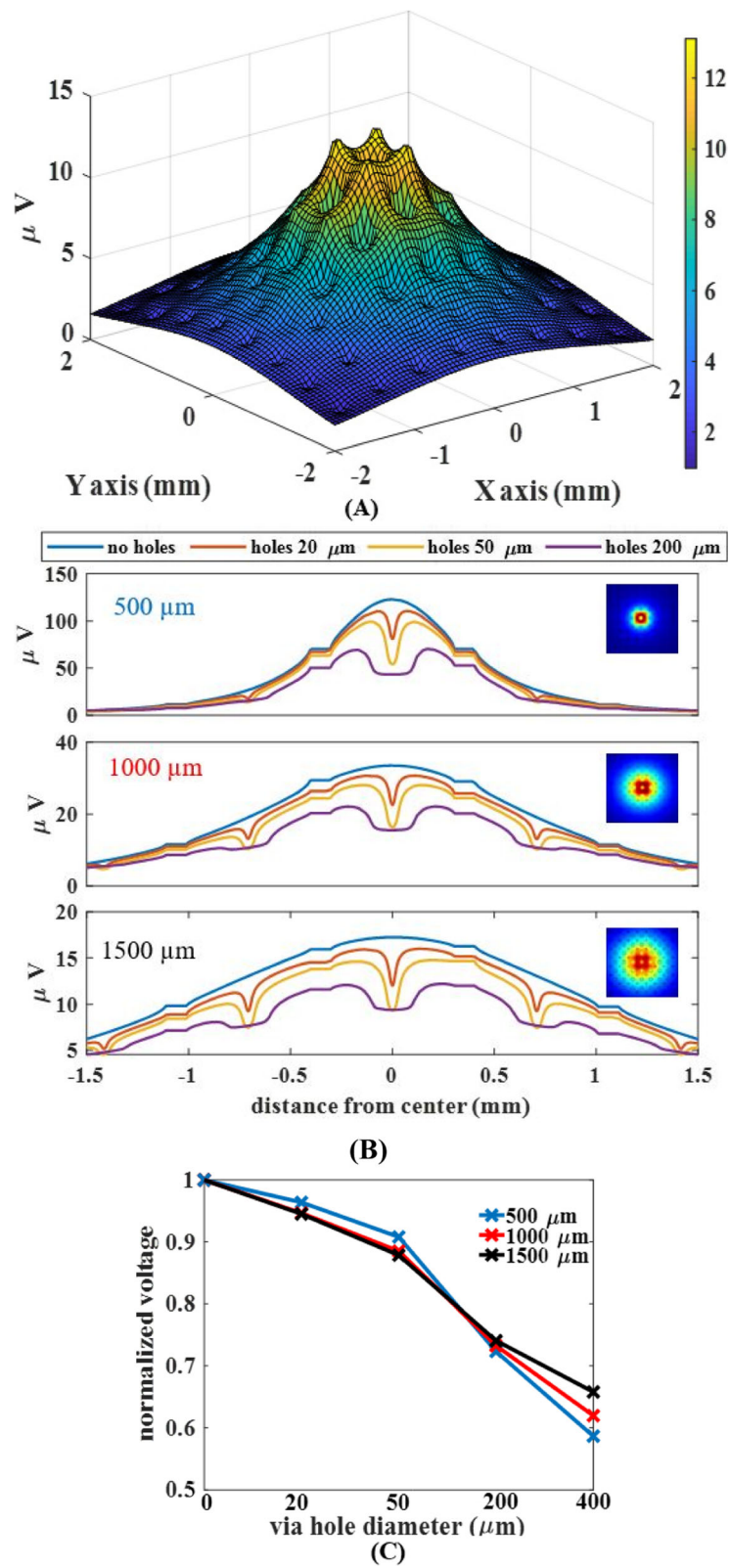


Fig. 5 (See legend on next page.)

(See figure on previous page.)

**Fig. 5** Voltage profiles recorded at the bottom surface of the array ( $4 \times 4$  mm) from neurons located at three different depths (500  $\mu\text{m}$ , 1000  $\mu\text{m}$ , and 1500  $\mu\text{m}$ ) for different via hole sizes. **A:** Surface mesh plot depicting the effects of the via holes (200  $\mu\text{m}$ ) on the voltage profile from a neuron located at a depth of 1500  $\mu\text{m}$  exactly beneath the geometric center of the array. **B:** Voltage profiles along the diagonal axis of the array that goes through the centers of the holes and contacts. **C:** Relative amplitudes (recorded at the contact locations that are closest to the via hole at the array center) for different via hole sizes. Each trace is normalized by the voltage for the substrate with no holes

The effect of the hole size was investigated for different neuron depths (Fig. 5). The 3D mesh plots in Fig. 5A resemble a spongy bed-like structure with a peak voltage at the horizontal coordinates of the source neuron. The voltage amplitudes decreased and spread wider for the neurons positioned deeper into the gray matter from the pia surface (Fig. 5B). The fractional voltage drops at the center of the holes were similar for all neuron depths, although the absolute values were smaller for deeper neurons. The electrode contacts introduced horizontal steps in the profile by forcing the local potential to the average of the voltages around them because of their high conductivity. Interestingly, the voltages at locations that are away from the via holes were also affected and deviated from the voltage profiles of the “no holes” case to increasing degrees with the hole size.

Normalized voltage profiles demonstrated an interesting interplay between the neuron depth and the hole size on the recorded amplitudes (Fig. 5C). The relative impact of the via holes was smaller first for the neuron closest to the surface (500  $\mu\text{m}$ ) and then larger than that of deeper neurons as the hole size was increasing. Thus, the curve is steeper for shallower neurons.

Next, the neuron was moved off-center and aligned with a contact on the diagonal axis (Neuron A in Fig. 2) in order to visualize the effects of asymmetry on the recorded signals (Fig. 6). The asymmetry induced in the voltage distribution due to the array edges closer to the neuron can be appreciated in the heat-plots of the top panel. The plots in the bottom panel resemble those in Fig. 5B except that there is a contact at the location of the voltage peak instead of a via hole. Unlike the plots of Fig. 5B, however, the positioning of the neuron produced a slight asymmetric in the voltage profiles, which was more pronounced with the neurons closer to the surface.

Next, we investigated spatial selectivity. Figure 7 illustrates the voltages recorded by the contact positioned directly above Neuron A from that neuron and also Neuron B, which is symmetrically positioned on the other side of the array center as shown in Fig. 2. Spatial Selectivity is defined by Equ. 1 where A and B are the voltages recorded from Neuron A and Neuron B respectively as marked by black dots in Fig. 7. Voltage profiles are slightly asymmetrical as expected. In this example for a specific neuron depth and hole size, the selectivity is 0.88.

Spatial selectivity is lower for neurons located deeper in the gray matter (Fig. 8). The presence of the holes lowers the selectivity with a stronger impact as the hole size is increasing when the distance between the neurons is large (2121  $\mu\text{m}$ , dash lines) regardless of the neuron depth. Paradoxically, the selectivity increases with increasing hole sizes initially when the inter-neuron distance is smaller (707  $\mu\text{m}$ ) before it drops for the larger hole size(s). Spatial selectivity is maximized at 200  $\mu\text{m}$  via-hole size for neuronal depths of 500  $\mu\text{m}$  and 1000  $\mu\text{m}$ , and at 50  $\mu\text{m}$  hole size for the deepest neuron (1500  $\mu\text{m}$ ).

## Discussion

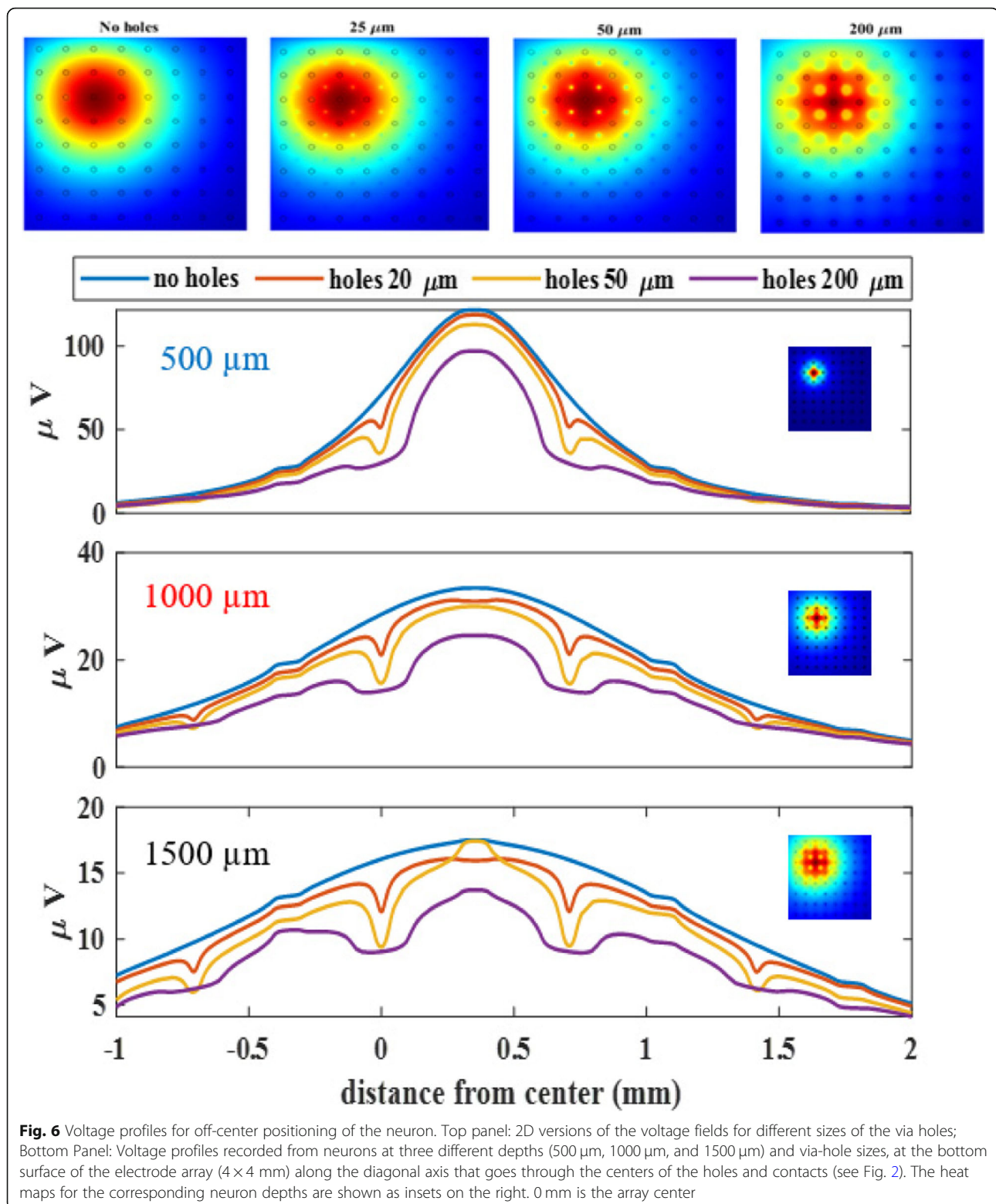
### Substrate size

The presence of the substrate blocks the currents flowing in the vertical direction and thus reduces the rate of voltage decline by distance from the neuron in that direction. The size of the electrode substrate clearly improves the recorded signal amplitudes especially if it is larger than the array-neuron distance. The signal amplitude saturates once the array dimensions are an order of magnitude larger than the depth of the neuron. The thickness of the human cortex varies between 1 and 4.5 mm and has an average thickness of 2.7 mm on the gyrus regions [16].

The human versions of the ECoG arrays are usually at least an order of magnitude larger than the deepest targets in the cortex. Thus, the clinical arrays that are larger than a few cm square should be able to maximize the signals even from the deepest neurons in the cortex due to this substrate effect. However, as the brain size is becoming smaller in smaller species like the rat and mouse, the cortex thickness does not scale down proportionally, and sometimes small arrays are preferred with dense arrangement of the contacts. As a practical value, one should be aware that the signal amplitudes may be reduced down to 79% (of the amplitudes recorded with a large array) when the substrate dimensions are in the same order as the depth of the targeted neurons (compare  $1 \times 1$  mm and  $4 \times 4$  mm arrays in Fig. 4).

### Holes size as a design parameter

Intuitively, the effect of the via holes should be the opposite to that of the substrate. We can anticipate that the presence of a large via hole in the substrate should cause some reduction of the recorded signals. That is,



the current flowing through the holes would increase the rate of decline in the extracellular voltage in the vertical direction. The simulations of the current study provided some general guidelines on how the signal

amplitudes vary with the hole size. The impact slightly depends on the depth of the targeted neurons for recording. As a practical guideline, 200  $\mu\text{m}$  holes will cause about 25% reduction in the recorded signals from the rat

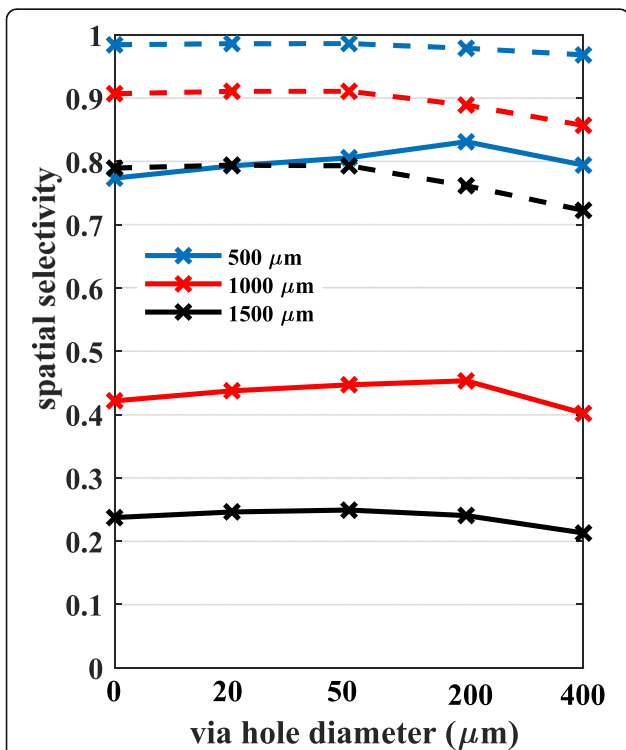
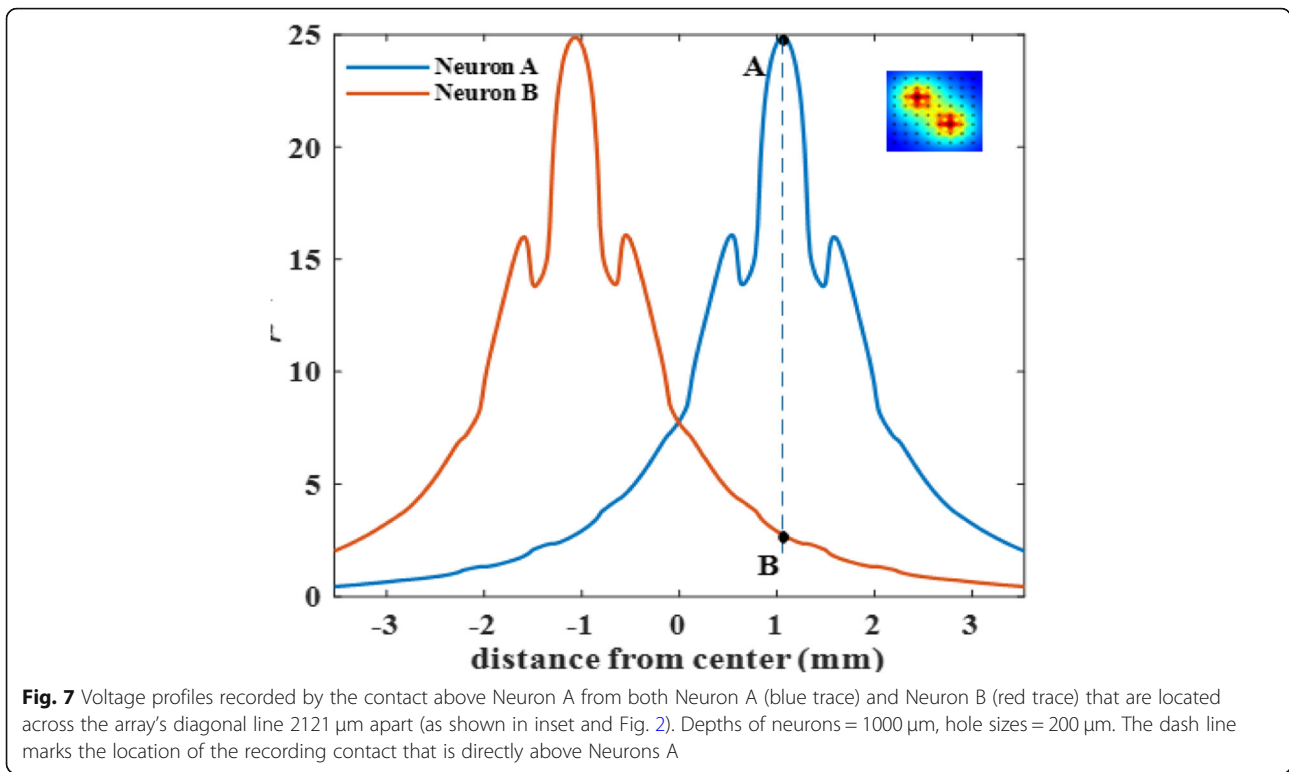


**Fig. 8** Spatial selectivity values calculated for neuron pairs located at different depths (500, 1000, and 1500  $\mu\text{m}$ ) and for different sizes of the via holes. The distance between Neuron A and B is either 707  $\mu\text{m}$  (solid lines) or 2121  $\mu\text{m}$  (dash lines) as shown in Fig. 2. In all cases, the signals were recorded at the contact that is aligned with Neuron A

cortex, regardless of the neuron depth, compared to the case without via holes (Fig. 5C). This hole size is about 40% of the contact pitch (500  $\mu\text{m}$ ). But, the signal deterioration will be stronger for shallower neurons if the via-hole size is larger than 200  $\mu\text{m}$ .

**Spatial selectivity**

If the inter-neuron distance is large (dash lines in Fig. 8), spatial selectivity is large to begin with but lowered by increasing amounts with the hole size and the neuron depth. For shallow neurons, the effect is negligibly small even at the largest hole size of 400  $\mu\text{m}$  (80% hole diam. / pitch ratio). For smaller inter-neuron distances (solid lines in Fig. 8), selectivity first increases with the hole size before the point of diminishing returns, which occurs at smaller via-hole sizes for deeper neurons. In general, it seems that inter-neuron distance and neuron depth have opposing effects on selectivity, and the hole size is a third parameter that can maximize selectivity at a point determined by the first two. Overall, potential improvement on selectivity by optimizing the hole size is marginal. Larger improvements in selectivity may be possible with alternative arrangements of the contacts and the holes on the substrate. Nonetheless, even this marginal gain in selectivity may provide the edge needed when multi-contact arrays are used for source localization in different layers of the brain cortex. Finally, we have to point out that micro vessels and connective tissue may grow through the perforating holes

over time in chronic implants [17]. This may significantly reduce the field effects induced by the presence of the holes due to somewhat higher resistivity of these tissues than the CSF, which would otherwise be filling the holes.

## Conclusions

Spatial selectivity of multi-contact neural recordings could be maximized by proper selection of the via-hole size. Increasing the spatial selectivity is analogous to reducing the inter-channel correlation and thus maximizing the information content of the multi-channel signals. The via-hole size could be leveraged as an optimization parameter to maximize the information content of neural recordings while maintaining sufficient signal amplitudes above the noise floor. Further investigation of this phenomenon is warranted within a larger parameter space and using more realistic neural models that include all neuronal compartments such as a dendritic tree, the soma, and an axon with realistic membrane currents and positions in the gray matter. The optimum via-hole size may also be different for different neuronal subtypes because of differences in their morphology and orientation, in addition to depth, in the gray matter.

## Abbreviations

ECoG: Electrocorticography;  $\mu$ ECoG: Micro-electrocorticography; FE: Finite element; BCI: Brain-computer interface; CSF: Cerebrospinal fluid

## Acknowledgements

Not applicable.

## Authors' contributions

M. Sahin conceptualized the original ideas. M. Sethia has developed the finite element model and produced the figures. Both authors have written the manuscript. Both authors have read and approved the final manuscript.

## Funding

Not applicable.

## Availability of data and materials

No biological data included in this publication. The finite element model can be made available upon request via email at [sahin@njit.edu](mailto:sahin@njit.edu).

## Declarations

### Ethics approval and consent to participate

Not applicable.

### Consent for publication

Not applicable.

### Competing interests

None.

Received: 27 September 2021 Accepted: 7 March 2022

Published online: 21 March 2022

## References

- Shokoueinejad M, et al. Progress in the field of Micro-Electrocorticography. *Micromachines* (Basel). 2019;10(1):62.
- Toda H, et al. Simultaneous recording of ECoG and intracortical neuronal activity using a flexible multichannel electrode-mesh in visual cortex. *Neuroimage*. 2011;54(1):203–12.
- Xie K, et al. Portable wireless electrocorticography system with a flexible microelectrodes array for epilepsy treatment. *Sci Rep*. 2017;7(1):7808.
- Rogers N, et al. Correlation structure in Micro-ECoG recordings is described by spatially coherent components. *PLoS Comput Biol*. 2019;15(2):e1006769.
- Wang X, et al. Mapping the fine structure of cortical activity with different micro-ECoG electrode array geometries. *J Neural Eng*. 2017;14(5):056004.
- Rouse AG, et al. Spatial co-adaptation of cortical control columns in a micro-ECoG brain-computer interface. *J Neural Eng*. 2016;13(5):056018.
- Slutzky MW, et al. Optimal spacing of surface electrode arrays for brain-machine interface applications. *J Neural Eng*. 2010;7(2):26004.
- Insanally M, et al. A low-cost, multiplexed  $\mu$ ECoG system for high-density recordings in freely moving rodents. *J Neural Eng*. 2016;13(2):026030–0.
- Bundy DT, et al. Characterization of the effects of the human dura on macro- and micro-electrocorticographic recordings. *J Neural Eng*. 2014;11(1):016006.
- Ordek G, Groth JD, Sahin M. Effect of anesthesia on spontaneous activity and evoked potentials of the cerebellar cortex. *Annu Int Conf IEEE Eng Med Biol Soc*. 2012;2012:835–8.
- Ordek G, Groth JD, Sahin M. Differential effects of ketamine/xylazine anesthesia on the cerebral and cerebellar cortical activities in the rat. *J Neurophysiol*. 2013;109(5):1435–43.
- Konerding WS, et al. New thin-film surface electrode array enables brain mapping with high spatial acuity in rodents. *Sci Rep*. 2018;8(1):3825.
- Sun FT, Morrell MJ, Wharen RE Jr. Responsive cortical stimulation for the treatment of epilepsy. *Neurotherapeutics*. 2008;5(1):68–74.
- Dreher JC, Grafman J. The roles of the cerebellum and basal ganglia in timing and error prediction. *Eur J Neurosci*. 2002;16(8):1609–19.
- Stoodley CJ, Stein JF. The cerebellum and dyslexia. *Cortex*. 2011;47(1):101–16.
- Fischl B, Dale AM. Measuring the thickness of the human cerebral cortex from magnetic resonance images. *Proc Natl Acad Sci U S A*. 2000;97(20):11050–5.
- Schendel AA, et al. A cranial window imaging method for monitoring vascular growth around chronically implanted micro-ECoG devices. *J Neurosci Methods*. 2013;218(1):121–30.

## Publisher's Note

Springer Nature remains neutral with regard to jurisdictional claims in published maps and institutional affiliations.

Ready to submit your research? Choose BMC and benefit from:

- fast, convenient online submission
- thorough peer review by experienced researchers in your field
- rapid publication on acceptance
- support for research data, including large and complex data types
- gold Open Access which fosters wider collaboration and increased citations
- maximum visibility for your research: over 100M website views per year

At BMC, research is always in progress.

Learn more [biomedcentral.com/submissions](https://biomedcentral.com/submissions)

